Density Functional Study on the Reaction Mechanism of Proton Transfer in 2-Pyridone: Effect of Hydration and Self-Association

Aiping Fu,*,† Hongliang Li,‡ Dongmei Du,† and Zhengyu Zhou†,§

Department of Chemistry, Qufu Normal University, Shandong, Qufu 273165, P. R. China; Max-Planck-Institut für Kohlenforschung, Mülheim an der Ruhr 45470, Germany; and State Key Laboratory of Crystal Materials, Shandong University, Shandong, Jinan, 250100, P. R. China

Received: October 10, 2004; In Final Form: December 9, 2004

The proton-transfer mechanism in the isolated, mono, dehydrated forms and dimers of 2-pyridone and the effect of hydration or self-assistance on the transition state structures corresponding to proton transfer from the keto form to the enol form have been investigated using B3LYP and BH-LYP hybrid density functional methods at the 6-311++G (2d, 2p) basis set level. The barrier heights for both H_2O-assisted and self-assisted reactions are significantly lower than that of the bare tautomerization reaction from 2-pyridone to 2-hydroxypyridine, implying the importance of the superior catalytic effect of H_2O and $(H_2O)_2$ and the important role of 2-pyridone itself for the intramolecular proton transfer. Long-range solvent effects have also been taken into account by using the continuum model (Onsager model and polarizable continuum model (PCM)) of water. The tautomerization energies and the potential energy barriers are increased both for the water-assisted and for the self-assisted reaction because of the bulk solvent, which imply that the tautomerization of PY becomes less favorable in the polar solvent.

Introduction

Proton-transfer reactions are important in many chemical and biological systems.[1−6] A particular type of proton transfer is one in which catalyst molecules can mediate the process by serving as a bridge that connects the donor and acceptor sites. For instance, in aqueous solution, one or more solvent water molecules may stabilize the transition state and therefore substantially lower the classical energy barrier to proton transfer. Another type of proton transfer is that the subject molecules may aggregate, and self-mediated proton transfer may take place. In this study, we examine the water-assisted and self-assisted tautomerization of 2-pyridone (PY) to 2-hydroxypyridine (HY).

The protomeric tautomerism of PY and HY is frequently considered to be the prototype for the oxo−hydroxy tautomerization process in heterocyclic compounds.[7−9] Some of the nucleic acid bases exhibit this type of lactim−lactam tautomerism, and it has been suggested many times that this might be at the origin of mutations.[10,11] Numerous studies on the tautomerization of PY and HY have been performed experimentally[12−22] as well as theoretically.[23−34] In the gas phase the tautomeric equilibrium has been the subject of many experimental studies ranging from low resolution (infrared, ultraviolet, X-ray photoelectron, multiphoton ionization, fluorescence excitation, and dispersed emission) spectroscopies[12−14,16] to rotationally resolved (laser-induced fluorescence and microwave) spectroscopies.[15,17] It has been reported that HY is more stable than PY by 2−3 kJ/mol in the gas phase. Also, the corresponding hydrogen-bonded system, $PY-H_2O/HY-H_2O$, has been studied in the gas phase by low resolution (time-of-flight mass spectrometry, emission spectroscopy, and infrared spectroscopy)[13,18,20,22] and high resolution (fluorescence excitation spectroscopy).[19] In the last report only $PY-H_2O$ has been observed. In liquid phase, both forms coexist in nonpolar solvents, while PY substantially dominates in a pure crystalline or in polar solvents.[35−37] As these results suggest, the tautomerization equilibrium depends inherently on the environment surrounding the molecule. In this respect, it is quite interesting to investigate the tautomerization of PY to HY by using molecular clusters as a microscopic model for the environment. Most ab initio calculations[28,30−34] to date have focused on the hydrogen-bonding interactions between the two tautomers and the water molecule or the spectra studies of them; only a few studies[23,24,29] have attempted to examine the proton-transfer mechanism of PY to HY. Field and Hiller[23] have used the 3-21G basis incorporating the CI expansion to investigate the proton-transfer mechanism of PY to HY. However, the lack of polarization functions in the basis set has made the results less reliable. Barone and Adamo[29] have investigated the mechanism of oxo/hydroxy tautomerization in 2-pyridone by means of the density functional /Hartree−Fock hybrid method using SVP and TZ2P basis sets. It was reported that the specific interactions with a single water molecule strongly enhance the reaction rate and shift the equilibrium toward the lactam form. Maris et al.[33] determined the relative stability of the two 1:1 complexes of PY and HY with water using density functional and ab initio calculations. Chou et al.[31] have investigated the conjugated dual hydrogen bonds mediating PY dimer tautomerization at the 6-31+G** basis set level employing the MP2 and HF methods. They presented the relative stability of the two isomerized dimers and also pointed out that the MP2 method leads to the reverse stability between the PY and HY dimer, which contradicted the experimental observations. To our knowledge, detailed and systematic ab initio investigations of the mechanism (such as the transition states) of the hydrogen bond assisted proton transfer reaction in 2-pyridone on high-level basis sets, especially those including

† Qufu Normal University.
‡ Max-Planck-Institut für Kohlenforschung.
§ Shandong University.
* Corresponding author. E-mail: faplhl@eyou.com.

10.1021/jp0453764 CCC: $30.25
Published on Web 02/02/2005

polarized and diffuse functions, have not been performed. Furthermore, regardless of many efforts to calculate the hydrogen-bonding effect and the relative total molecular electronic energy, focus on the tautomeric equilibria and the calculation of the free energy for these hydrogen bond species is relatively lacking.

Therefore, in this paper, we will investigate the water-assisted and self-assisted proton-transfer mechanism of 2-pyridone to 2-hydroxypyridine. The following systems are studied: (i) proton transfer via an intramolecular mechanism; (ii) a mechanism involving one water molecule as a bifunctional catalyst in an intermediate cyclic structure; (iii) a mechanism involving two bridged water molecules; (iv) tautomeric interconversion within a self-associated dimer. The present study has been undertaken with the objective to adhere to the following questions: (i) the effect of hydration or self-association on the relative stabilities of different tautomers and their geometries; (ii) the structure of the transition state corresponding to the keto−enol tautomerism and the effect of hydration or self-association on the nature of the transition states; (iii) the barrier height for the keto−enol tautomerization and the influence of the hydrogen bond on the barrier height; (iv) the interaction energy of the hydrogen-bonded complexes of two tautomers.

In the second part, as compared to the isolated gas-phase results, we have carried out the study of the bulk solvent effect on the kinetics and the thermodynamics of the tautomerization reactions corresponding to the above four mechanisms. The influence of the bulk solvent on the structures, the relative stability, and the activation barrier of different systems have been analyzed.

Computational Methods

The ground-state geometries of the reactants, transition states, and products for the tautomerization of the isolated, mono, dehydrated, and self-associated complexes of PY are optimized using the density functional theory (DFT) with the BH-LYP[38] and the most popular B3LYP[38,39] methods applying the 6-311++G (2d, 2p) basis sets. All geometries of local minimum and transition states are optimized without any symmetry restrictions. Vibrational frequencies have been obtained at the same level for characterization of stationary points and zero-point energy (ZPE) corrections. The validity of the transition state structures is further validated by the IRC. Since the inclusion of the BSSE correction has minor importance to the binding energy for the 6-311++g(2d,2p) basis set for the B3LYP method,[40,41] this correction is not discussed. Long-range effects of the solvent water medium are taken into account by means of a dielectric continuum represented by the Onsager model[42] and the polarizable continuum model (PCM).[43] We have used both the Onsager and the PCM model for geometry optimizations and the energy calculations. The continuum calculations were done with a dielectric constant $\epsilon = 78.39$ at 298.15 K and 0.1 MPa. All calculations are carried out with the Gaussian 98 program package.

Results and Discussion

Geometries. Although the structures of the equilibrium geometry were discussed in detail at varied levels for the bare and water-monomer-catalyzed process of the proton-transfer reaction of PY;[23,24,27,29] in the present paper, we put forward what we believe are now the most accurate results as obtained from high-level calculations, especially for the tautomerization of the dehydrated forms and dimers of PY. Furthermore, though the tautomerization of PY and HY has been of interest to chemists for a very long time, the geometries of the transition states for the water-assisted and self-assisted proton transfer reaction have only been reported at the STO-3G and 3-21G levels of calculation. Figure 1 shows the geometries of the reactants, transition states, and products involved in the $(H_2O)_2$ and self-assisted proton-transfer reactions at B3LYP/6-311++G-(2d,2p) level. The geometries of the direct and H_2O-assisted reactions are also illustrated in Figure 1 for the comparison purposes. The geometric parameters of PY, HY, and the corresponding transition state are collected in Table 1. Since the intramolecular angles and distances of the water complexes are essentially the same as in the bare molecules, only some of them are shown in Tables 2 and 3, together with the intermolecular water−PY geometrical parameters. The parameters for the self-assisted tautomerization process are listed in Table 4.

Recently, Piacenza and Grimme[44] have carried out the systematic quantum chemical study of DNA−base tautomers including pyridone and hydroxypyridine. They mentioned that the corrected MP2 method named SCS-MP2 works very well for the PY/HY system, and the tautomerization energy is only 0.1 kcal/mol above the corresponding QCISD(T) value. They also presented that the BH-LYP method can give the correct energy order for PY tautomers and outperforms the commonly used B3LYP method. To test the reliability of this method in these proton-transfer systems, we have also performed the optimizations at BH-LYP/6-311++G(2d,2p) level. As was pointed out, this method yields relatively short bond lengths compared with the B3LYP and MP2 methods. However, the overall deviations from the available experiment data of PY/HY monomer employing different methods are similar, and the computational method does not seem to have a large influence on the molecular geometries. For simplicity, the geometric data calculated at BH-LYP/6-311++G(2d,2p) level are listed as Supporting Information, and the discussion about the geometries is restricted to the B3LYP method.

For the direct proton-transfer mechanism (PY→ TS → HY), comparison of geometries for the two stationary points of planar PY and HY shows, as expected, that all the bond lengths sensibly change as the tautomerization proceeds. In particular, the N_1-C_2 bond length reduces from 1.408 to 1.324 Å, while the C_2-O_4 distance increases from 1.224 to 1.355 Å in going from PY to HY. The shape of the ring also changes with two C−N bond lengths and four C−C bond lengths become very nearly equal. Hence, the oxo group is converted to a hydroxy group, and a cyclic conjugated system with aromatic character is established. With regard to the transition state connecting the keto form to the enol form by intramolecular proton transfer of PY, it appears to hold a coplanar four-membered ring. From the examination of the structural changes from reactant to product, it can be seen that the N_1-C_2 and C_2-O_4 bond lengths of the TS are intermediate, being 1.359 and 1.289 Å, respectively. This is consistent with the breaking of the CO double bond and the corresponding formation of the π CN bond. Specifically, for tautomerization to occur, the PY must undergo large structural changes that are energetically expensive. The $N_1C_2O_4$ bond angle is compressed from an equilibrium value of 120.0° to 105.5° at B3LYP/6-311++ G(2d,2p) level, a 12% decrease. The NH bond is then stretched from 1.009 to 1.295 Å, an increase of 28% to reach the transition state. In other words, the structural changes reflect the process of the formation of a new bond (O−H) and the rupture of an old bond (N−H). This means H atom transfers from the N atom to the O atom.

For H_2O-assisted tautomerization (PYW → TSW → HYW), as pointed out by Held and Pratt,[19] the most stable geometry of

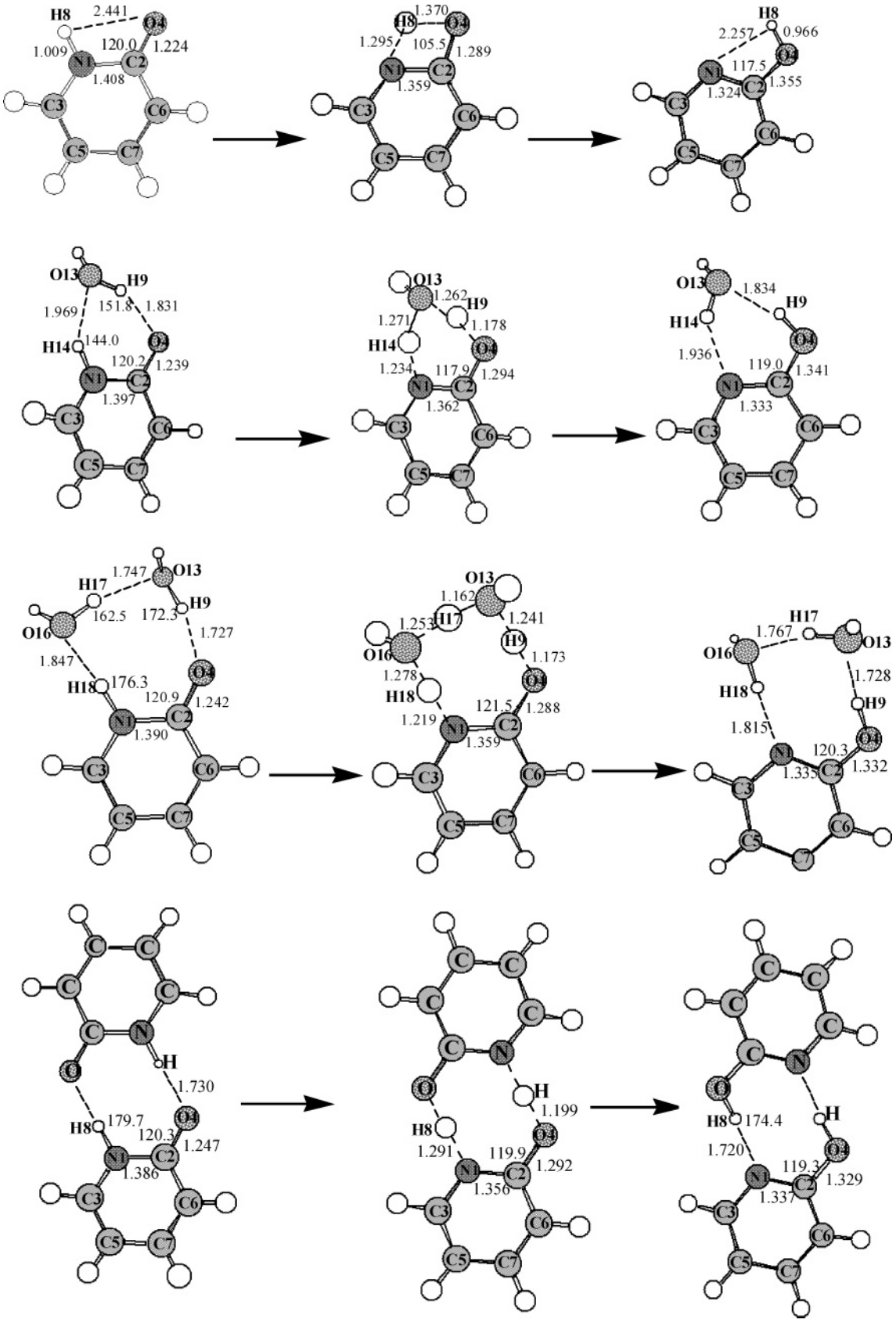

Figure 1. Mechanism for proton transfer in isolated, monohydrated, dehydrated, and self-associated dimer of 2-pyridone in the gas phase at B3LYP/6-311++G(2d,2p).

the reactant PYW is the cyclic double-hydrogen-bonded structure. The water molecule acts simultaneously as a proton donor and acceptor. This is a nearly coplanar six-membered-ring structure with a O−H bond of H_2O stretching out of the plane. Two hydrogen-bonding distances are 1.969 and 1.831 Å. This complex is stabilized by two nonlinear hydrogen bonds with computed $O_{13}-H_9\cdots O_4$ and $N_1-H_{14}\cdots O_{13}$ angles of 151.8° and 144.0°. (The values deduced by Held and Pratt from their

TABLE 1: Geometric Parameters for PY, TS, and HY in the Gas Phase and in Water Medium Employing the SCRF Onsager Model and PCM Model (B3LYP)[a]

	PY			TS			HY		
	A	B	C	A	B	C	A	B	C
N_1-C_2	1.408	1.401	1.393	1.359	1.356	1.352	1.324	1.324	1.327
N_1-C_3	1.361	1.363	1.360	1.336	1.338	1.337	1.339	1.340	1.343
C_2-O_4	1.224	1.234	1.242	1.289	1.301	1.304	1.355	1.358	1.354
C_2-C_6	1.448	1.442	1.440	1.406	1.401	1.400	1.398	1.397	1.399
C_3-C_5	1.358	1.358	1.361	1.382	1.382	1.384	1.385	1.385	1.385
C_5-C_7	1.423	1.419	1.418	1.406	1.403	1.404	1.396	1.396	1.397
C_6-C_7	1.361	1.365	1.366	1.382	1.386	1.386	1.382	1.383	1.383
N_1-H_8	1.009	1.009	1.019	1.295	1.299	1.324	2.257	2.245	2.287
H_8-O_4	2.441	2.448	2.465	1.370	1.359	1.364	0.966	0.966	0.978
$N_1-C_2-O_4$	120.0	120.0	120.0	105.5	105.1	105.2	117.5	117.2	117.9
$N_1-C_2-C_6$	113.2	113.2	114.0	120.3	120.5	120.9	124.0	124.1	123.9
$C_2-C_6-C_7$	121.6	121.6	121.3	116.6	116.6	116.3	117.5	117.4	117.6
$C_5-C_7-C_6$	121.5	121.5	121.3	122.0	121.9	121.8	119.6	119.5	119.6
$C_3-C_5-C_7$	118.0	117.9	118.0	118.6	118.7	118.7	118.0	118.0	118.0
$C_2-N_1-C_3$	125.3	125.4	124.9	123.2	123.1	123.0	117.7	117.6	117.6
$H_8-N_1-C_2$	114.5	114.9	115.9	75.1	75.0	75.5	56.2	56.5	56.0

[a] Lengths in angstroms and angles in degrees. A: gas phase; B: Onsager model; C: PCM model.

TABLE 2: Relevant Geometric Parameters of PYW, TSW, and HYW in the Gas Phase and in Water Medium Employing the SCRF Onsager Model and PCM Model (B3LYP)[a]

	PYW			TSW			HYW		
	A	B	C	A	B	C	A	B	C
N_1-C_2	1.397	1.392	1.388	1.362	1.355	1.354	1.333	1.332	1.332
N_1-C_3	1.357	1.361	1.3259	1.344	1.347	1.345	1.342	1.343	1.344
C_2-O_4	1.239	1.247	1.251	1.294	1.309	1.312	1.341	1.348	1.350
C_2-C_6	1.440	1.435	1.433	1.414	1.406	1.406	1.402	1.400	1.400
C_3-C_5	1.361	1.360	1.362	1.373	1.373	1.374	1.382	1.381	1.383
C_5-C_7	1.419	1.417	1.416	1.406	1.404	1.404	1.398	1.397	1.397
C_6-C_7	1.363	1.366	1.367	1.374	1.377	1.378	1.380	1.381	1.382
N_1-H_{14}	1.020	1.017	1.018	1.234	1.183	1.208	1.936	1.885	1.977
$H_{14}-O_{13}$	1.969	2.124	2.104	1.271	1.343	1.307	0.980	0.985	0.979
N_1-O_{13}	2.858	2.981	2.966	2.421	2.447	2.435	2.793	2.775	2.817
$O_{13}-H_9$	0.981	0.986	0.981	1.262	1.373	1.333	1.834	1.878	1.814
H_9-O_4	1.831	1.762	1.807	1.178	1.103	1.125	0.982	0.979	0.984
O_4-O_{13}	2.735	2.712	2.741	2.395	2.435	2.418	2.776	2.814	2.765
$N_1-C_2-O_4$	120.2	120.0	120.0	117.9	117.4	117.2	119.0	118.7	118.5
$H_{14}-O_{13}-H_9$	78.6	72.0	73.5	81.5	78.3	79.1	79.5	76.5	80.2
$O_{13}-H_9-O_4$	151.8	160.5	157.9	158.1	159.1	159.2	159.6	159.0	161.7
$N_1-H_{14}-O_{13}$	144.0	140.7	141.0	150.1	151.2	151.1	144.6	148.9	142.4
$H_{14}-N_1-C_2$	114.8	115.0	115.9	106.5	107.9	107.5	107.4	108.0	107.6

[a] Lengths in angstroms and angles in degrees. A: gas phase; B: Onsager model; C: PCM model.

experimental data are 139.6° and 146.2°, respectively.[19]) The computed N−H···O angle is in good agreement with the experimental value, whereas the O−H···O angle is larger than the corresponding experimental value. This agrees with the result of Del Bene at the MP2/6-31+G(d,p) level[28] and of Dkhissi at the 6-31++G(d,p) level using the B3LYP and B3PW91 methods.[32] The calculated intermolecular distances O···O (2.74 Å) and O···N (2.86 Å) are in good agreement with the experiment data of 2.77 and 2.86 Å, respectively. Surveying the calculated results of PY and PYW is that changes in the monomer geometries upon hydration are relatively minor for most geometric parameters. Monohydration induces a small elongation of the C═O bond and a contraction of the C−N bond. Other bond lengths involved in the hydrogen bonding slightly lengthen. The maximum bond length change is less than 0.015 Å at the B3LYP/6-311++G(2d,2p) level. The binding energy of PY and H_2O is 44.9 (34.8) kJ/mol (the value shown in parentheses includes the ZPE correction). This agrees with the results by Dkhissi using MP2 and B3LYP methods at the

TABLE 3: Relevant Geometric Parameters of PY2W, TS2W, and HY2W in the Gas Phase and in Water Medium Employing the SCRF Onsager Model and PCM Model (B3LYP)

	PY2W			TS2W			HY2W		
	A	B	C	A	B	C	A	B	C
N_1-C_2	1.390	1.387	1.384	1.359	1.352	1.353	1.335	1.334	1.334
N_1-C_3	1.357	1.359	1.358	1.349	1.354	1.352	1.345	1.346	1.347
C_2-O_4	1.242	1.248	1.253	1.288	1.306	1.303	1.332	1.339	1.341
C_2-C_6	1.439	1.435	1.434	1.420	1.409	1.412	1.406	1.403	1.403
C_3-C_5	1.361	1.361	1.362	1.370	1.368	1.370	1.380	1.379	1.381
C_5-C_7	1.418	1.416	1.415	1.406	1.405	1.405	1.398	1.397	1.398
C6−C7	1.364	1.366	1.367	1.371	1.375	1.375	1.378	1.379	1.380
N_1-H_{18}	1.028	1.026	1.029	1.219	1.139	1.171	1.815	1.793	1.833
$H_{18}-O_{16}$	1.847	1.869	1.851	1.278	1.400	1.348	0.990	0.993	0.988
N_1-O_{16}	2.873	2.894	2.878	2.495	2.539	2.517	2.803	2.783	2.818
$O_{16}-H_{17}$	0.985	0.982	0.982	1.253	1.255	1.269	1.767	1.746	1.773
$H_{17}-O_{13}$	1.747	1.783	1.784	1.162	1.163	1.152	0.982	0.984	0.983
$O_{13}-H_9$	0.987	0.992	0.985	1.241	1.417	1.320	1.728	1.777	1.713
$O_{16}-O_{13}$	2.703	2.735	2.739	2.397	2.405	2.405	2.706	2.694	2.714
H_9-O_4	1.727	1.689	1.741	1.173	1.068	1.116	0.990	0.986	0.992
O_4-O_{13}	2.708	2.679	2.724	2.414	2.485	2.436	2.711	2.754	2.696
$N_1-C_2-O_4$	120.9	120.8	120.5	121.5	121.4	121.2	120.3	120.1	119.8
$H_{18}-N_1-C_2$	117.5	117.4	117.7	122.0	121.7	122.2	129.9	129.5	130.4
$N_1-H_{18}-O_{16}$	175.6	177.5	176.0	175.6	177.0	176.5	174.9	174.7	174.1
$H_{18}-O_{16}-H_{17}$	95.5	96.3	95.6	94.1	92.7	92.5	90.3	91.6	90.2
$O_{16}-H_{17}-O_{13}$	162.5	162.3	163.1	153.2	167.9	167.1	158.7	160.5	159.2
$H_9-O_{13}-H_{17}$	97.4	94.2	94.6	99.8	96.9	98.6	102.5	98.9	102.0
$O_4-H_9-O_{13}$	178.5	175.4	174.7	178.5	178.1	177.7	171.4	170.4	170.1
$C_2-O_4-H_9$	131.7	131.9	131.4	120.1	117.9	118.7	113.6	113.1	113.3

[a] Lengths in angstroms and angles in degrees. A:gas phase; B: Onsager model; C: PCM model.

TABLE 4: Relevant Geometric Parameters of $(PY)_2$, $(TS)_2$, and $(HY)_2$ in the Gas Phase and in Water Medium Employing the SCRF Onsager Model and PCM Model (B3LYP)

	PY_2		$(TS)_2$			HY_2	
	A	C	A	B	C	A	C
N_1-C_2	1.386	1.382	1.356	1.360 (1.348)	1.355 (1.348)	1.337	1.336
N_1-C_3	1.354	1.356	1.346	1.342 (1.350)	1.346 (1.350)	1.343	1.346
C_2-O_4	1.247	1.255	1.292	1.285 (1.307)	1.299 (1.311)	1.329	1.337
C_2-C_6	1.437	1.433	1.418	1.424 (1.409)	1.418 (1.408)	1.405	1.403
C_3-C_5	1.363	1364	1.373	1.378 (1.371)	1.377 (1.372)	1.380	1.381
C_5-C_7	1.416	1.415	1.405	1.404 (1.404)	1.403 (1.403)	1.399	1.399
C_6-C_7	1.366	1.368	1.373	1.373 (1.375)	1.376 (1.377)	1.378	1.380
N_1-H_8	1.039	1.035	1.291	1.506 (1.193)	1.468 (1.219)	1.720	1.711
H_8-O	1.730	1.770	1.199	1.066 (1.306)	1.083 (1.276)	1.006	1.008
N−O	2.768	2.805	2.488	2.570 (2.497)	2.549 (2.492)	2.722	2.715
$N_1-C_2-O_4$	120.3	119.8	119.9	119.8 (120.1)	119.3 (119.8)	119.3	118.9
$N_1-C_2-C_6$	114.9	115.2	118.8	119.0 (119.4)	119.5 (119.6)	122.0	122.3
$C_2-C_6-C_7$	121.0	120.8	119.7	119.8 (119.3)	119.6 (119.2)	118.5	118.4
$C_5-C_7-C_6$	121.1	121.1	120.3	120.1 (120.3)	120.0 (120.3)	119.7	119.7
$C_3-C_5-C_7$	117.8	117.9	117.6	117.4 (117.9)	117.6 (117.9)	117.8	117.9
$C_2-N_1-C_3$	124.2	124.2	121.0	120.2 (121.2)	120.1 (121.0)	118.6	118.6
$H_8-N_1-C_2$	116.6	116.5	120.4	120.1 (120.9)	120.9 (121.1)	123.6	123.7
N_1-H_8-O	179.7	180.0	176.0	176.5 (175.0)	176.3 (174.8)	174.4	174.0
H_8-O-C	123.3	123.7	115.7	114.2 (116.5)	114.2 (115.8)	111.5	111.4

[a] Lengths in angstroms and angles in degrees. A: gas phase; B: Onsager model; C: PCM model.

6-31++G** level.[32] TSW is the transition state for the water-monomer-catalyzed tautomerization. The role of the water is to serve as a proton relay. TSW shows two concerted hydrogen-transfer processes occurring antilockingwise along the ringy skeleton. The breaking of the N_1-H_{14} bond is accompanied by the H_{14} atom transfers from N_1 to O_{13} and another H_9 in H_2O from O_{13} to O_4, forming product HYW. For HYW, it is also the double-hydrogen-bonded systems with the two hydrogen bonds 1.936 and 1.834 Å, respectively. The binding energy is 39.3 (29.0) kJ/mol. A comparison of the geometrical parameters of isolated and hydrated HY suggests that hydration also

influences the geometrical parameters in the vicinity of the intermolecular hydrogen-bonding region. The more pronounced changes are a lengthening of the C═N bond and a shortening of the C−O bond while it is reverse for the keto form. Such phenomena can be attributed due to hydrogen bond accepting and donating properties of the oxo and hydroxy groups, respectively. As shown in Figure 1 and Table 2, the tendency of the geometrical parameter changes of the water-assisted proton transfer reaction is similar to that of the bare tautomerization of PY. However, in comparison with the normal tautomerization, the obvious difference is that the NCO angle has to be compressed by only 2.3° (for PY→ HY is 14.5°). We may predict the large reduction in the classical energy barrier from the normal to the water-catalyzed case attributed to the water acting as a catalyst through the stabilization of the transition state. Most of the energy saving is achieved because the NCO angle need not be compressed to such a large extent as the normal reaction. At the same time, the N−H bond lengthening decreased by about 25% which is another factor contributing to the lower energy barrier of reaction PYW → TSW → HYW.

Similar to the H_2O-monomer-assisted process, for the $(H_2O)_2$-catalyzed mechanism (PY2W → TS2W → HY2W), the reaction also started by the formation of the PY2W, which involves a coplanar eight-membered ring due to the formation of the three hydrogen bonds. In this complex, it is the water dimer that acts as both the proton donor and proton acceptor. As evident from Figure 1, the water dimer fits quite nicely into the N−H and C═O region. The calculations show that $N_1-H_{18}\cdots O_{16}$ (176.3°) and $O_4-H_9\cdots O_{13}$ (172.3°) bonds are nearly linear hydrogen bonds. The most nonlinear hydrogen bond is found in the bonded water dimer, i.e., the $O_{16}-H_{17}\cdots O_{13}$ bond (162.5°). These results confirm the assumptions by Held and Pratt.[19] The computed intermolecular $N_1\cdots O_{16}$ and $O_{13}\cdots O_{16}$ distances are 2.87 and 2.70 Å, which are in very good agreement with the experimentally determined distances of 2.85 and 2.67 Å, respectively. The intermolecular distance $O_4\cdots O_{13}$ is underestimated by about 0.07 Å in comparison with the experimental value. Compared with the geometric parameters of PYW, $H_{18}-O_{16}$ and O_4-H_9 hydrogen bonds are 1.847 and 1.727 Å, respectively, about 0.1 Å shorter than those in the PYW. Moreover, Del Bene[28] and Dkhissi[32] have pointed out that the intermolecular distance $O_{13}\cdots O_{16}$ in the PY2W complex is at least 0.2 Å shorter than this distance in the water dimer. This most remarkable change is due to the formation of a stronger bond to PY and reflects the cooperative effect in this system. Also, as expected, the bond lengths of O−H and N−H are larger in this complex than the values of those bonds in PYW, which also reflects the strong cooperative effect in PY2W. TS2W is the transition state for the $(H_2O)_2$-catalyzed tautomerization. In the reaction process, two H_2O molecules are involved in assisting the passage of the H atom from PY to HY. TS2W shows three concerted hydrogen-transfer processes occurring along the ring skeleton. This means that three new bonds have been formed, and three old bonds are prone to rupture in the proton-transfer process. Similar to PY2W, HY2W is also planar with respect to the heavy atoms. Three hydrogen bonds are present in this complex. Compared with HYW, there is also a strong cooperative effect in HY2W.

As discussed above, from Figure 1, we can see the framework of the PY monomer changes greatly in TS than that in TSW and TS2W. In addition, the $N_1H_8O_4$ angle is 104.5° in TS and $N_1H_{14}O_{13}$ and $O_{13}H_9O_4$ angles are 150.1° and 158.1° in TSW, whereas $N_1H_{18}O_{16}$, $O_{16}H_{17}O_{13}$, and $O_{13}H_9O_4$ are 174.8°, 153.2°, and 178.0° in TS2W. The less deformation from the linear structure causes the H atom easier to transfer in proceeding of PY2W → TS2W → HY2W and PYW → TSW → HYW than in proceeding of PY→ TS → HY. So the intimate involvement of water can assist the H atom transfer.

For the PY self-associated mechanism, the optimized geometries of the stationary points and transition state at the B3LYP/6-311++G(2d,2p) level are also illustrated in Figure 1, and the parameters are shown in Table 4. Similar to the water-catalyzed reactions, the reactant of the centrosymmetric PY dimer also forms a coplanar eight-membered ring via two equivalent N−H···O═C hydrogen bonds. The association energy between two PY monomers is 80.0 (74.9) kJ/mol. Experimentally, the association energy of the PY dimer has been reported to be dependent on the solvent polarity, e.g., 24.6 kJ/mol in $CHCl_3$,[45] 61.8 kJ/mol in CCl_4,[46] and 64.8 kJ/mol in benzene.[47] The lower association energy in the high-polar medium can be rationalized by the calculated dipole moment of 4.4 D for the PY monomer with respect to that of zero for the PY dimer. Therefore, for the PY monomer the dipole−dipole interaction plays an important role in polar media, resulting in additional stabilization energy. Accordingly, it is reasonable to predict that the binding energy of the PY dimer in the gas phase should be close to that of 65.0 kJ/mol measured in benzene. The calculated binding energy of 74.9 kJ/mol in the gas phase correlates reasonably well with the experimental results. This is in good agreement with the discussion by Chou[31] and Dkhissi.[32] $(PY)_2$ has also been previously studied by different spectroscopic techniques, which have yielded precise rotational constants and N···O hydrogen bond distances, as well as inter- and intamolecular vibrational frequencies.[21,48] The availability of accurate gas-phase data allows us to access the reliability of our calculation. The experimentally determined angle C═O···N is 121.8 ± 0.5°. Our calculations predict the value of 123.3° within this range. The B3LYP/6-311++G(2d,2p) calculations give a N···O distance of 2.77 ± 0.03 Å, in excellent agreement with the experimental value (2.79 Å) derived by Held and Pratt.[48] The hydrogen bond is predicted to be close to linear with the angle N−H···O of 179.6°, and the hydrogen bond distance H···O is 1.73 Å. Furthermore, formation of the two antiparallel hydrogen bonds leads to quite substantial changes of the intramolecular bond lengths, especially in the vicinity of the amide group. The calculations predict that upon dimerization both the N−H single bond and the C═O double bond increase by 0.03 and 0.02 Å, respectively; on the other hand, the C−N single bond contracts by 0.02 Å. These results suggest a cooperative change in the electronic configuration of PY mediated by the conjugated dual hydrogen bond formation. These changes are similar in size and magnitude to the lengthening of the C═O bond and shortening of the C−N bond measured for formamide from the experimental electron diffraction and X-ray analyses of the monomer and hydrogen-bonded polymer.[49] Upon comparison of the data of PYW and $(PY)_2$, the significant change in relative bond distances for the PY dimer shows that there must be stronger hydrogen bond interactions in the self-association complex than that in the water-associated complex. This can be confirmed by the larger binding energies of PY dimer than PYW. $(TS)_2$ is the transition state for this self-assisted tautomerization. It is noteworthy that the transitions state of the double-proton-transfer process has C_{2h} symmetry because the optimization without any symmetry restriction could not localized the TS. This double-proton-transfer process occurs in a concerted and synchronous way with the breaking of the N−H bond and the formation of the O−H bond. $(PY)_2$ isomerized to $(HY)_2$. Similarly, $(HY)_2$

TABLE 5: Computed B3LYP, BH-LYP/6-311++G(2d,2p), and Experimental Ground State Rotational Constants (MHz)

	computed			experimental[a,b]		
	A	B	C	A	B	C
PY	5679 (5762)	2798 (2851)	1875 (1907)	5644	2794	1869
PYW	4010 (4079)	1397 (1410)	1038 (1049)	3997	1394	1035
PY2W	2610 (2645)	895 (900)	669 (674)	2581	896	669
$(PY)_2$	2019 (2060)	316 (318)	273 (276)	2014	319	276

[a] Reference 19. [b] Reference 48. Values in parentheses computed using the BH-LYP method.

also appears to be a cyclic double-hydrogen-bonded structure; the hydrogen bond distance is 1.720 Å, and the binding energy is 63.7 (59.5) kcal/mol. From the analysis of the relative distance for several crucial bonds with respect to the HY monomer, we can see, apparently, both an increase and a decrease of the double-bond character are on the order of PY dimer > HY dimer, which corresponds to the decreasing trend of the association energy. Through the comparison of the electronegativity of the N−H nitrogen and the O−H oxygen, the C═O oxygen, and the pyridinal nitrogen, it can be deduced that more electron density is shifted from the amino proton to the carbonyl oxygen in the PY dimer than from the hydroxyl proton to the pyridinal nitrogen, resulting in stronger hydrogen bond formation in the PY dimer. As shown in Figure 1, the framework of PY in the double proton transfer does not change as greatly as that in bare PY → HY. Also, the NHO angle is quasi-linear (176.0°), causing the H atom easier to transfer.

Experimental data on rotational constants for isolated, monohydrated, and dehydrated forms of 2-pyridone and 2-pyridone dimers are also available. Table 5 collects the rotational constants calculated at the B3LYP and BH-LYP/6-311++G(2d,2p) levels as well as the experimental data. The B3LYP calculations can yield very satisfactory *B* and *C* constants, but relatively less good agreement with *A*, especially for the PY monomer and dehydrated PY. However, we note again that the accuracy of rotational constants obtained in this work is better than that obtained by Del Bene[28] for PY−water complexes at the MP2/6-31+G(d,p) level and in good agreement with that reported by Müller[34] for PY dimers at the MP2/6-311++G(d,p) level. It is worth noting that the BH-LYP method yields the rotational constants in bad agreement with the experiment. Besides the molecular parameters, the overall quality of the B3LYP method is further confirmed by a comparison between the computed and experimental rotational constants of different subject complexes, while it is not the case for the BH-LYP method.

Energetics. The thermodynamic parameters for four tautomerization reaction processes at B3LYP and BH-LYP/6-311++G(2d,2p) levels are summarized in Table 6 and Table 7, respectively. The values in parentheses are including zero-point vibrational energy (ZPE) corrections. Also, the Gibbs free energy barrier heights are also presented in these two tables.

From the tables we can see the direct proton transfer is characterized by a high activation energy. The barrier governing the tautomerization is 157.6 kJ/mol, the zero-point energy correction further decreasing the activation energy to 144.1 kJ/mol at the B3LYP/6-311++G(2d,2p) level. This is in good agreement with the results by Barone and Adamo at the MP2/SVP and B3LYP/SVP level,[29] whereas those of Field and Hiller[23] obtained at the CISD/3-21G level using HF/3-21G geometries are relatively high (183 kJ/mol). However, since the superiority of the DFT methods has been doubted by several recent studies[6,50,51] that some commonly used gradient-corrected functionals give barriers to low compared with post-HF methods

TABLE 6: Calculated Activation Energies, Gibss Free Energy Barrier Heights, and Changes of Electronic Energy and Free Energy for the Proton Transfer Reactions in the Isolated, Monohydrated, Dihydrated, and Self-Associated Forms of Pyridone at the B3LYP/6-311++G(2d,2p) Level in Gas Phase and in Solution Phase (kJ/mol)

	gas phase			solution phase				
	$\Delta E^{\ddagger}$	$\Delta G^{\ddagger}$	ΔE	ΔG	$\Delta G^{\ddagger a}$	ΔG^{a}	$\Delta G^{\ddagger b}$	ΔG^{b}
PY → HY	157.6 (144.1)	144.6	1.5 (1.1)	1.5	150.1	15.2	176.1	15.4
PYW → HYW	63.1 (47.2)	52.3	7.1 (6.9)	7.5	52.4	13.1	70.2	14.6
PY2W → HY2W	67.6 (45.4)	52.6	12.5 (12.1)	12.8	52.5	15.8	74.6	15.7
$(PY)_2$ → $(HY)_2$	40.0 (18.7)	24.1	19.2 (17.6)	18.4	24.4	18.4	43.5	23.8

[a] Onsager model. [b] PCM model.

TABLE 7: Calculated Activation Energies, Gibss Free Energy Barrier Heights, and Changes of Electronic Energy and Free Energy for the Proton Transfer Reactions in the Isolated, Monohydrated, Dihydrated, and Self-Associated Forms of Pyridone at the BH-LYP/6-311++G(2d,2p) Level in Gas Phase and in Solution Phase (kJ/mol)

	gas phase			solution phase				
	$\Delta E^{\ddagger}$	$\Delta G^{\ddagger}$	ΔE	ΔG	$\Delta G^{\ddagger a}$	ΔG^{a}	$\Delta G^{\ddagger b}$	ΔG^{b}
PY → HY	176.6 (162.6)	163.2	-4.2 (−4.6)	-4.2	167.7	7.9	193.5	10.2
PYW → HYW	77.6 (60.5)	65.9	3.1 (2.9)	3.5	64.7	7.4	84.7	13.4
PY2W → HY2W	85.5 (61.4)	69.2	9.4 (9.0)	9.7	68.6	12.3	94.3	12.9
$(PY)_2$ → $(HY)_2$	48.4 (23.1)	27.0	12.7 (11.8)	12.2	30.1	12.2	51.2	21.6

[a] Onsager model. [b] PCM model.

and experiments. To access the reliability of the popular B3LYP method to this proton-transfer system, we use the smallest bare tautomerization reaction process as the best candidates. Hence, we have also carried out the MP2 calculations at 6-31+G(d,p), 6-31++G(d,p), 6-311++G(d,p), and 6-311++G(2d,2p) for comparison purposes. B3LYP calculations are also performed at other basis sets. The calculated activation energies and the energy differences between two tautomers at different levels are listed in Table 8. The table shows the calculated activation energy values using MP2 and B3LYP methods at different basis set levels are in good agreement with each other, and there is no evidence of the B3LYP method to underestimate the reaction barrier heights. Hence, the following calculations based on the B3LYP method at the 6-311++G(2d,2p) basis set level are of sufficient accuracy for further discussion.

Inclusion of a water molecule drastically reduces the activation energy to 47.2 kJ/mol using the B3LYP method, which is about one-third of the barrier height governing the intramolecular tautomerization. The calculated value of $\Delta E^{\ddagger}$ is relatively lower than that of the previous study by Field at the CISD/3-21G level[23] and Barone at the B3LYP/SVP level,[29] who have not considered the ZPE correction. A substantial reduction in the barrier to tautomerization suggested that proton transfer would be easily facilitated by the presence of a water molecule. In the crystal of isocytosine, the presence of water vapor increases proton migration, which leads to an increased amount of electric current pass through it.[52] Such phenomena are indicative of the fact that the presence of water vapor decreases the barrier height of proton transfer. Further inclusion of one more water molecule located between the N−H and C═O site as a bridge yields the activation energy of 45.4 kJ/mol by the B3LYP method. The only available post-HF data in the literature for the two bridged water molecules assisted tautomerization are those of Field and Hiller (obtained at the CISD/3-21G level, using HF/3-21G

TABLE 8: Calculated Activation Energies, Gibss Free Energy Barrier Heights, and Changes of Electronic Energy for the Direct Proton Transfer Reaction of Pyridone at Different Levels in Gas Phase (kJ/mol)

	MP2			B3LYP		
	$\Delta E^{\ddagger}$	$\Delta G^{\ddagger}$	ΔE	$\Delta E^{\ddagger}$	$\Delta G^{\ddagger}$	ΔE
6-31+G(d,p)	151.4 (138.4)	139.4	−8.6 (−8.0)	154.3 (140.8)	141.3	1.9 (1.5)
6-31++G(d,p)	151.3 (139.1)	144.6	−8.7 (−7.1)	154.2 (140.8)	141.2	1.8 (1.4)
6-311++G(d,p)	149.3		−11.8	158.8 (145.1)	145.6	3.6 (3.3)
6-311++G(2d,2p)	150.0		−10.1	157.7 (144.1)	144.6	1.5 (1.1)

geometries),[23] which give an energy barrier of 13 kJ/mol lower than that of water-monomer-assisted reaction. With respect to our calculation, the second water molecule in the bridging site has no significant effect on the reduction of the activation energy in comparison with the monohydrated process. Similar results have been found for the proton transfer in the hypoxanthine tautomers by Shukla et al.[53] In conclusion, these results suggest that the proton transfer would be easily facilitated by the presence of one or two water molecules.

Table 7 indicates that the BH-LYP method at the same basis set level predicts the ZPE corrected activation energy for the bare tautomerization and the water-assisted tautomerization to be 13−18 kJ/mol higher than those of the B3LYP method. This may be due to the large fraction of HF exchange (50%) in the BH-LYP method. However, except for the absolute values, a similar trend can be derived both from B3LYP and BH-LYP methods.

For the PY dimer tautomerization, the energy barrier also decreases dramatically. The B3LYP predicted barrier height of 40 kJ/mol is much lower than the only available data (52 kJ/mol) of Field and Hiller.[23] The inclusion of zero-point energy correction further decreases the height of the barrier by about 21 kJ/mol. The energy barrier also decreased by about 87% compared with the bare tautomerization. The BH-LYP method gives similar results with the activation energy being 23.1 kJ/mol. All the results indicate that the cyclic dimer of PY is also helping to accelerate the proton transfer.

The general picture emerging from the above computations is that the high-energy barrier basically rules out the possibility of a direct proton-transfer reaction in the ground state. Since PY has NH donor and C═O acceptor H-bonding sites, it can form stable complexes with other species such as water or itself. The complex formation is predicted to greatly decrease the barrier height. This phenomenon is popular in many systems.

The electronic and free energy changes calculated by B3LYP and BH-LYP methods for four tautomerization reactions are also listed in Tables 6 and 7. On the other hand, the calculated energy differences between two isolated tautomers at a different basis set level using MP2 and B3LYP methods are also presented in Table 8. Those tables show that the ZPE correction has a slight effect on the magnitude of the relative energy of the different tautomers. A considerable number of quantum chemical calculations have been performed on the subject of the relative stability between PY and HY.[23,27,29,31,44] It has been found that MP2 calculations overestimate the stability of HY with respect to PY, whereas density functional methods provide different results on the tautomeric relative energies depending on the employed basis sets. The experimental energy difference value between the isolated tautomers, $\Delta E = E_{HY} - E_{PY}$, is −3.2 kJ/mol.[17] The calculated values are $\Delta E_{MP2} = -10.1$ kJ/mol, $\Delta E_{B3LYP} = 1.1$ kJ/mol, and $\Delta E_{BH-LYP} = -4.6$ kJ/mol at the 6-311++G(2d,2p) level, respectively (as shown in Tables 7 and 8). MP2 and BH-LYP methods predict the correct energetic order for the two isolated tautomers with the BH-LYP method yielding good performance for the reaction energy and the MP2 method overestimating the energy difference. Although the B3LYP method predicts incorrectly that in the gas phase the NH tautomer is more stable than the OH one, the absolute error at this level is only about 4.3 kJ/mol. As pointed out by Maris et al.[33] and Piacenza et al.,[44] corrections up to the MP4 order or calculations at QCISD(T)/TZV(2df,2dp) level can improve the ab initio values to −3.6 or −4.2 kJ/mol, which are much closer to the experimental data. But those methods are unpractical to the large system. The less absolute error and the cost-effective character for computation made the two DFT methods to be the best choice of this system.

The effect of hydration is to favor the stability of the keto form over the enol form by 6.9 (2.9) kJ/mol using the B3LYP (BH-LYP) method. The most accurate value available in the literature is 1.27 kJ/mol at the MP4(SDTQ)//MP2/6-311++G** level,[33] while in the same paper, MP2/6-311++G** predicted HYW has a 5.61 kJ/mol lower energy than PYW because of its overestimation of the stability of HY. The reaction energy can also be deduced through another indirect method. The above discussion has shown that the hydrogen bonds with a water molecule in PYW are 5.6 kJ/mol stronger than in HYW at the B3LYP level, which stabilizes the energy of PYW more to increase the tautomerization energy. If we consider these binding energies reliable, we can apply them as correction to the experimental ΔE value relative to the isolated tautomers, and we can estimate the energy difference between the hydrated ones as about $\Delta E = E_{HYW} - E_{PYW} = 2.4$ kJ/mol (in favor of PY). MP4 and BH-LYP give best predictions, and MP2 has bias toward the relative stability order. Although our B3LYP method slightly overestimates the concentration of the keto form, the effect of the water molecule in displacing the tautomeric equilibrium is essentially correct. Taking into account the estimated value of 2.4 kJ/mol, the equilibrium constant and the relative distribution between PYW and HYW can be calculated using the standard formular $K = e^{-\Delta G/RT}$, where the calculations were performed at 298.15 K. The two tautomers would coexist in the gas phase, and the enol form is shown to be present in about 38% of the total tautomeric forms of the molecule.

Although the effect of the second water molecule in the bridging site on the kinetics of tautomerization is not significant, dihydration further stabilized the keto form by about 5−6 kJ/mol, in comparison with the monohydrated one using two DFT methods. These changes are large enough to significantly affect the equilibrium concentration for keto and enol forms. Even if we considered that the B3LYP method has overestimated the energy difference, the dyhydration would further shift the tautomeric equilibrium to the keto form, and PY2W would substantially dominate in this situation.

Also for the PY dimer tautomerizatin, the calculated ΔE and ΔG are 17.6 (11.8) and 18.4 (12.2) kJ/mol employing the B3LYP (BH-LYP) method. As expected, the tautomerization energy of B3LYP may be overestimated. The calculated binding energy of $(PY)_2$ is higher than that of $(HY)_2$ by about 15.4 kJ/mol. If we consider these values reliable, we can also apply them as correction to the experimental ΔE value relative to the isolated tautomers, and we can estimate the energy difference of $(PY)_2$ and $(HY)_2$ about 9.0 kJ/mol. This large energy

difference indicates that $(HY)_2$ will not be detected in the self-aggregation state. X-ray crystallography has revealed that PY is the only tautomer present in the crystal state and supported our calculation.

In conclusion, the high activation energy has ruled out the possibility of the direct intramolecular proton transfer in single PY; then the possible reaction mechanism for the tautomerization reaction in the gas phase may be the intermolecular proton transfer in short living (collisional) hydrogen-bond dimers because of the much lower activation energy of the self-assisted tautomerization. The multiple hydrogen bond formation, as proposed, not only dynamically catalyzes the proton transfer reaction but also thermodynamically manipulates the overall tautomeric equilibrium.

Effects of Long-Range Solvent Environment. Through the above discussion, it is not surprising that one or two intimate water molecules can affect the proton-transfer reaction mechanism of PY by assisting the passage of the H atom from one tautomeric form to the other. However, these theoretical studies are still for the gas phase. What are the possible effects of the nonintimate water molecules as the surrounding environment to the characteristic of the potential energy surface such as the tautomerization energy and the barrier height for the proton transfer? In this section, the long-range solvent effect has been taken into account by using the self-consistent reaction field (SCRF) theory. In the reaction field theory, the solute in a cavity is surrounded by a polarizable medium with a dielectric constant. A dipole in the solute induces a dipole in the medium, and the electric field applied to the solute by the solvent dipole will interact with the solute dipole to produce net stabilization. The cavity radius is the adjustable parameters, and the choice of the radius has been discussed extensively. In the Onsager model,[42] the radius was calculated from the molecular volume of the optimized structure in the gas phase, on the assumption that the structure is spherical, and added by 0.5 to consider the surrounding solvent molecules. In the polarizable continuous model (PCM) model,[43] the cavity used was of molecular shape and was built by interlocking spheres. The radii of the spheres were obtained by scaling the atomic van der Waals radii. The surface of each sphere was divided in 60 triangular tesserae (default value) for the calculation of the surface-charge distribution. In the present paper, we have employed these two (SCRF) models: the Onsager model and the PCM model to determine the solvent effects on the geometric and energetic parameters of four tautomerization reaction processes.

We start the discussion from the change of the geometrical parameters of four tautomerism systems from gas phase to solution phase. (The values in solution phase at the B3LYP level are also listed in Tables 1−4, and the BH-LYP values are shown in the Supporting Information.) For the PY → HY tautomerization reaction, the dipole moments of PY, TS, and HY in the gas phase are 4.4, 3.5, and 1.3 D at the B3LYP/6-311++G-(2d,2p) level, respectively. As expected, the calculated changes in structure in going from the gas phase to water are small for most of the bond lengths and bond angles. In particular, the introduction of a solvent reaction field has little effect on the calculated geometry of 2-hydroxypyridine. In contrast, significant changes in molecular geometry are predicted for the more polar keto tautomer and TS. The calculated C_2-N_1 and C_2-O_4 bond lengths of PY (TS) are found to be altered by 0.007 (0.003) Å and 0.010 (0.012) Å in going from the gas phase to the solvent of water using the Onsager model, while the values are 0.015 (0.007) Å and 0.018 (0.015) Å using the PCM model. The lengthening of the C−O bond and shortening of the C−N bond correspond to a small increase in the weight of the dipolar resonance structure. This is in good agreement with Wong et al. at the HF level.[27] On the other hand, compared with those in the gas phase at TS, the breaking N−H increases about 0.004 (0.029) Å and the forming O−H decreases about 0.011 (0.006) Å with the Onsager (PCM) model. The position of the proton at the TS is closer to the oxygen atom, which means that the transition state is later in solution than in gas phase.

For PYW → HYW, the dipole moments of PYW, TSW, and HYW are 3.6, 3.8, and 2.6 D in the gas phase. In PYW, similar to PY, the C_2-O_4 bond lengthens about 0.008 (0.012) Å and the C_2-N_1 bond shortens about 0.005 (0.009) Å employing the Onsager (PCM) model. The main discrepancies between the gas phase and the solution phase are that the $H_{14}\cdots O_{13}$ hydrogen bond is lengthened by 0.155 (0.135) Å, while $O_4\cdots H_9$ is shortened by 0.069 (0.024) Å. Differences in other bond lengths and bond angles between the gas phase and solution phase results are negligible. In TSW, there also have great changes in the region of the intermolecular hydrogen bonding. In addition to the C−O lengthening (0.015 or 0.018 Å) and the C−N shortening (0.007 or 0.008 Å), the N_1-H_{14} and O_4-H_9 are shortened by 0.051 (0.026) and 0.069 (0.053) Å, while $H_{14}-O_{13}$ and $O_{13}-H_9$ are lengthened by 0.072 (0.036) and 0.111 (0.071) Å using the Onsager (PCM) model. These changes in the H bond lengths result in the separation of the partial charges of TSW to increase the dipole moment (from 3.8 D in the gas phase to 6.48 (6.0) D in the solution phase). The NPA charge of the $O_{13}-H$ moiety of TS is 0.54*e* in the gas phase and 0.60-(0.57)*e* in medium of water by the Onsager (PCM) model. The TS structure in a polar solvent has more ion-pair character than in the gas phase. The results are consistent with the tautomerization reaction of formamide.[5] In HYW, the changes mainly reflect at C_2-O_4 (lengthened by 0.007 and 0.009 Å), N_1-H_{14} (shortened by 0.051 Å using the Onsager model and lengthened by 0.041 Å using the PCM model) and $O_{13}-H_9$ (lengthened by 0.044 Å by the Onsager model and shortened by 0.020 Å by the PCM model). Other geometric parameters of the solution phase and the gas phase are very similar.

For PY2W → HY2W, the dipole moments of PY2W, TS2W, and HY2W are 3.04, 3.06, and 2.06 D in the gas phase. For PY2W, the changes of the C_2-O_4 (0.006 and 0.011 Å) and C_2-N_1 bond (0.003 and 0.006 Å by two SCRF models) further decrease in comparison with that of PY and PYW in gong from the gas phase to solution phase. At the same time, the changes of the three hydrogen bond distance are also less than that of PYW. For example, $O_{16}\cdots H_{18}$ lengthens by 0.022 and 0.004 Å using the Onsager and PCM model, respectively, $H_{17}\cdots O_{13}$ lengthens by 0.036 and 0.037 Å, and $H_9\cdots O_4$ shortens by 0.038 Å by the Onsager model and lengthens by 0.014 Å by the PCM model. For TS2W, there are also great changes of the geometries in going from gas phase to solution phase. In addition to the changes of C_2-N_1 and C_2-O_4, N_1-H_{18} shortens by 0.080 and 0.048 Å and $H_{18}-O_{16}$ lengthens by 0.122 and 0.070 Å by two SCRF models. These changes mean that proton transfer of H_{18} is much delayed in solution phase. The changes of $O_{16}-H_{17}$ and $O_{13}-H_{17}$ are less than 0.002 Å. $O_{13}-H_9$ lengthens by 0.176 and 0.079 Å while H_9-O_4 shortens by 0.105 and 0.057 Å using the Onsager and PCM model, respectively. These changes indicate that proton transfer of H_9 is more advanced in solution phase than in gas phase. Similar with TSW, these changes in the H-bond lengths also result in the separation of the partial charges of TS2W to increase the dipole moment (from 3.06 D in gas phase to 7.4 (5.5) D in solution phase). For HY2W, as

expected, the changes also take place in the region of the intermolecular hydrogen bonding.

With respect to the PY self-assisted tautomerization reaction, the global dipole moments of $(PY)_2$ and $(HY)_2$ are zero since they have C_{2h} symmetry, and this gives zero reaction field in the Onsager SCRF model using spherical cavity so that there would be no energetic stabilization. The optimized geometric parameters in solution phase using the PCM model for $(PY)_2$ and $(HY)_2$ are summarized in Table 4. Similar to the change of the hydrated PY tautomers, the effect of the bulk solvent on the geometry of the self-associated dimers mainly reflects on the change of the hydrogen bond distance. In $(PY)_2$, the H_8-O distance lengthens about 0.04 Å while there is less variation in $(HY)_2$. For the $(TS)_2$, the geometry of C_{2h} symmetry has been optimized in solution. In addition to the Ag symmetry imaginary frequency, the Bu frequency becomes imaginary in water. This indicates that the TS with C_{2h} symmetry is not a real transition state. The real transition state structure in the medium with the water dielectric constant was recalculated using the Onsager and PCM model. The two SCRF methods all indicate that it has C_s symmetry. The geometric parameters are listed in Table 4. In this transition state, the values of $r(N-H)$ and $r(O-H)$ are 1.506 (1.193) and 1.066 (1.306) Å employing the Onsager model, while 1.468 (1.219) and 1.083 (1.276) Å by the PCM model. The H_8 proton attached initially on N_1 is already transferred to O, and the second proton is between O_4 and N. This indicates the first proton moves earlier than the second as the reaction proceeds, and thus two protons are transferred asynchronously. Furthermore, the reaction proceeds smoothly from reactant to product. This suggested that the two protons are transferred concertedly but asynchronously in water.

For four tautomerization processes, although the BH-LYP method yields relatively shorter intramolecular bond distances and longer intermolecular bond distances, it can also predict a similar trend of the geometric changes in going from gas phase to the solution phase with the B3LYP method.

Now, we pay our attention to the energetic parameters. The reaction energies and activation barriers in solution phase for the four reacting systems using PCM and Onsager models are also listed in Table 6 (B3LYP) and Table 7 (BH-LYP). These two tables show that inclusion of the nonspecific solvent has a significant effect on the tautomerization energies with both Onsager and PCM models. The bulk solvent stabilizing the molecule with the higher dipole moment increased the energy difference between the keto and enol forms, especially for the bare and water-monomer-assisted process. Two SCRF models give the results in good agreement with each other employing the B3LYP method, while at the BH-LYP level, PCM yields a larger energy difference than the Onsager model. It is noteworthy that the solvent has a significant effect on the proton-transfer activation energies by the PCM model while it has little effect by the Onsager model for both the B3LYP and BH-LYP methods. Barriers for the four tautomerization process increased at least 20 kJ/mol using the PCM model. These results suggested that the water-assisted and self-assisted tautomerization is not facilitated by providing polar environments. The specific water molecule can reduce the barrier height for the multiproton transfer to assist the tautomerization of 2-pyridone, however, the polar medium tends to increase the barrier height and the reaction energy of the water-assisted and self-assisted tautomerization.

Conclusion

We have performed a comprehensive study of the proton transfer mechanism in the isolated, mono, and dehydrated forms and dimers of 2-pyridone in the gas phase and in the solution phase at B3LYP and BH-LYP/6-311++G(2d,2p) level. The BH-LYP method can give better energy differences for the keto and enol tautomers, but the predicted rotational constants are in really bad agreement with the experimental values. B3LYP predicts a wrong energetic order for the isolated tautomers. However, it gives a small deviation. The good performance of B3LYP method to predict the geometric parameters, rotational constants, and hydrogen-bonding effects indicates that it is still practical for those proton-transfer systems. Although there are differences in the absolute values for the two DFT methods, the general trends are same both in the gas phase and in water medium. Both one or two specific water molecules and PY itself can stabilize the keto form in the gas phase by forming the stronger hydrogen bonds. Furthermore, the bulk solvent can also shift the tautomerization equilibrium to the keto form. These results are consistent with the experimental findings, which indicate that 2-pyridone is the most stable tautomer in polar solvent. On the other hand, the barrier heights for both H_2O-assisted and self-assisted reactions are significantly lower than that of the bare tautomerization reaction from 2-pyridone to 2-hydroxypyridine, while the activation energies for all the systems are increased with the water medium, and therefore the bare, water-assisted and self-assisted tautomerization becomes less favorable using the PCM model. There is another thing should also be noted that multiple proton transfer occurred concertedly and synchronously both in the gas phase and in solution in the water-assisted tautomerization process. For the self-assisted process, the double proton transfer is also concerted and synchronous with the transition state has C_{2h} symmetry in the gas phase, while in the water medium, the symmetry of the transition state changes to C_s and the double proton transfer occurs asynchronously by both the Onsager model and polarizable continuum model.

Acknowledgment. This work was supported by the Natural Science Foundation of Shandong Province (Z2002F01), the State Key Laboratory Foundation of Crystal Material, and the National Natural Science Foundation of China (29673025). We also thank the Qufu Normal University Research Fund for financial support.

Supporting Information Available: BHLYP/6-311++G(2d,2p) optimized geometric parameters for four tautomerization processes (Table S1−S4). This material is available free of charge via the Internet at http://pubs.acs.org.

References and Notes

(1) Coll, M.; Frau, J.; Vilanova, B.; Llinas, A.; Donoso, *Int. J. Chem.* **1999**, *2*, 18.
(2) Madeja, F.; Havenith, M. *J. Chem. Phys.* **2002**, *117*, 7162.
(3) Alavi, S.; Thomsom, L. D. *J. Chem. Phys.* **2002**, *117*, 2599.
(4) Bell, R. L.; Truong, T. N. *J. Chem. Phys.* **1994**, *101*, 10442.
(5) Kim, Y.; Lim, S.; Kim, H. J.; Kim, Y. *J. Phys. Chem. A* **1999**, *103*, 617.
(6) Lim, J.-H.; Lee, E. K.; Kim, Y. *J. Phys. Chem. A* **1997**, *102*, 2233.
(7) Krebs, C.; Hofmann, H. J.; Kölher, H. J.; Weiss, C. *Chem. Phys. Lett.* **1980**, *69*, 537.
(8) Kwiatkowski, J. S.; Zielinski, T. J.; Rein, R. *Adv. Quantum Chem.* **1986**, *18*, 85.
(9) Kwiatkowski, J. S.; Barlett, R. J.; Person, W. B. *J. Am. Chem. Soc.* **1988**, *110*, 2353.
(10) Pullman, B.; Pullman, A. *Adv. Heterocycl. Chem.* **1971**, *13*, 77.
(11) Topal, M. D.; Fresco, J. R. *Nature (London)* **1976**, *263*, 285.
(12) Brown, R. S.; Tse, A.; Vederas, J. C. *J. Am. Chem. Soc.* **1980**, *102*, 1174.
(13) Nimlos, M. R.; Kelley, D. F.; Bernstein, E. R. *J. Phys. Chem.* **1989**, *93*, 643.
(14) Smets, J.; Maes, G. *Chem. Phys. Lett.* **1991**, *187*, 532.

(15) Held, A.; Champagne, B. B.; Pratt, D. W. *J. Chem. Phys.* **1991**, *95*, 8732.
(16) Nowak, M. J.; Lapinski, L.; Fulara, J.; Les, A.; Adamowicz, L. *J. Phys. Chem.* **1992**, *96*, 1562.
(17) Haterley, L. D.; Brown, R. D.; Godfrey, P. D.; Pierlot, A. P.; Caminati, W.; Damiani, D.; Melandri, S.; Favero, L. B. *J. Phys. Chem.* **1993**, *97*, 46.
(18) Florio, G. M.; Gruenloh, C. J.; Quimpo, R. C.; Zwier, T. S. *J. Chem. Phys.* **2000**, *113*, 11143.
(19) Held, A.; Pratt, D. W. *J. Am. Chem. Soc.* **1993**, *115*, 9708.
(20) Matsuda, Y.; Ebata, T.; Mikami, N. *J. Chem. Phys.* **1999**, *110*, 8397.
(21) Müller, A.; Talbot, F.; Lentwyler, S. *J. Chem. Phys.* **2000**, *112*, 3717.
(22) Matsuda, Y.; Ebata, T.; Mikami, N. *J. Chem. Phys.* **2000**, *113*, 573.
(23) Field, M. J.; Hiller, I. H. *J. Chem. Soc., Perkin Trans. 2* **1987**, 617.
(24) Adamo, C.; Barone, V.; Loison, S.; Minichino, C. *J. Chem. Soc., Perkin Trans. 2* **1993**, 697.
(25) Moreno, M.; Miller, W. H. *Chem. Phys. Lett.* **1990**, *171*, 475.
(26) Barone, V.; Adamo, C. *Chem. Phys. Lett.* **1994**, *226*, 399.
(27) Wong, M. W.; Wiberg, K. B.; Frisch, M. J. *J. Am. Chem. Soc.* **1992**, *114*, 1645.
(28) Del Bene, J. E. *J. Phys. Chem.* **1994**, *98*, 5902.
(29) Barone, V.; Adamo, C.*J. Phys. Chem.* **1995**, *99*, 15062.
(30) Dkhissi, A.; Houben, L.; Smets, J.; Adamowicz, L.; Maes, G. *J. Mol. Struct.* **1999**, *484*, 215.
(31) Chou, P. T.; Wei, C. Y. *J. Phys. Chem. B* **1997**, *101*, 9119.
(32) (a) Dkhissi, A.; Adamowicz, L.; Maes, G. *Chem. Phys. Lett.* **2000**, *324*, 127. (b) Dkhissi, A.; Ramaekers, R.; Houben, L.; Adamowicz, L.; Maes, G. *Chem. Phys. Lett.* **2000**, *331*, 553.
(33) Maris, A.; Ottaviani, P.; Caminati, W. *Chem. Phys. Lett.* **2002**, *360*, 155.
(34) Müller, A.; Losada, M.; Leutwyler, S. *J. Phys. Chem. A* **2004**, *108*, 157.
(35) Beak, P.; Fry, F. S. *J. Am. Chem. Soc.* **1973**, *95*, 1700.
(36) Kuzuya, M.; Noguchi, A.; Okuda, T. *J. Chem. Soc., Chem. Commum.* **1984**, 435.
(37) Scanlan, M. J.; Hillier, I. H.; Macdowell, A. A. *J. Am. Chem. Soc.* **1983**, *105*, 3568.
(38) Becke, A. D. *J. Chem. Phys.* **1993**, *98*, 5648. Becke, A. D. *J. Chem. Phys.* **1993**, *98*, 1372.
(39) Lee, C.; Yang, W.; Parr, R. G. *Phys. Rev. B* **1988**, *37*, 785.
(40) Fu, A. P.; Du, D. M.; Zhou, Z. Y. *Chem. Phys. Lett.* **2003**, *377*, 537.
(41) Fu, A. P.; Du, D. M.; Zhou, Z. Y. *J. Mol. Struct. (THEOCHEM)* **2003**, *623*, 315.
(42) Onsager, L. *J. Am. Chem. Soc.* **1936**, *58*, 1486.
(43) (a) Miertus, S.; Scrocco, E.; Tomasi, *J. Chem. Phys.* **1981**, *55*, 117. (b) Cossi, M.; Mennucci, B.; Tomasi, J. *Chem. Phys. Lett.* **1994**, *228*, 165.
(44) Piacenza, M.; Grimme, S. *J. Comput. Chem.* **2004**, *25*, 83.
(45) Hammes, S. G.; Park, A. C. *J. Am. Chem. Soc.* **1969**, *91*, 956.
(46) Fujimoto, A.; Inuzuka, K. *Spectrochim. Acta, Part A* **1985**, *41*, 1471.
(47) Inuzuka, K.; Fujimoto, A *Bull. Chem. Soc. Jpn.* **1982**, *55*, 2537.
(48) Held, A.; Pratt, D. W. *J. Chem. Phys.* **1992**, *96*, 4869.
(49) Jeffrey, G. A.; Saenger, W. *Hydrogen Bonding in Biological Structures;* Springer: Berlin, 1991.
(50) Wei, D. Q.; Proynov, E. I.; Milet, A.; Salahub, D. R. *J. Phys. Chem. A* **2000**, *104*, 2384.
(51) Kim, Y. *J. Am. Chem. Soc.* **1996**, *118*, 1522.
(52) (a) Skaric, V.; Lacan, G.; Skaric, D. *J. Chem. Soc., Perkin Trans. 1* **1977**, 757. (b) Thomas, J. M.; Evans, J. R. N.; Lewis, T. *J. Discuss. Faraday Soc.* **1971**, *51*, 73.
(53) Shukla, M. K.; Leszczynski, J. *J. Phys. Chem. A* **2000**, *104*, 3021.